

High-speed AFM images of thermal motion provide stiffness map of interfacial membrane protein moieties

*Johannes Preiner^{†, ‡, *}, Andreas Horner[‡], Andreas Karner[†], Nicole Ollinger[‡], Christine Siligan[‡], Peter Pohl^{‡, §}, and Peter Hinterdorfer^{†, ‡, §}.*

[†]Center for Advanced Bioanalysis GmbH, Gruberstrasse 40, 4020 Linz

[‡]Institute of Biophysics, Johannes Kepler University Linz, Gruberstrasse 40, 4020 Linz

Corresponding Author

* Correspondence to: Johannes.Preiner@cbl.at

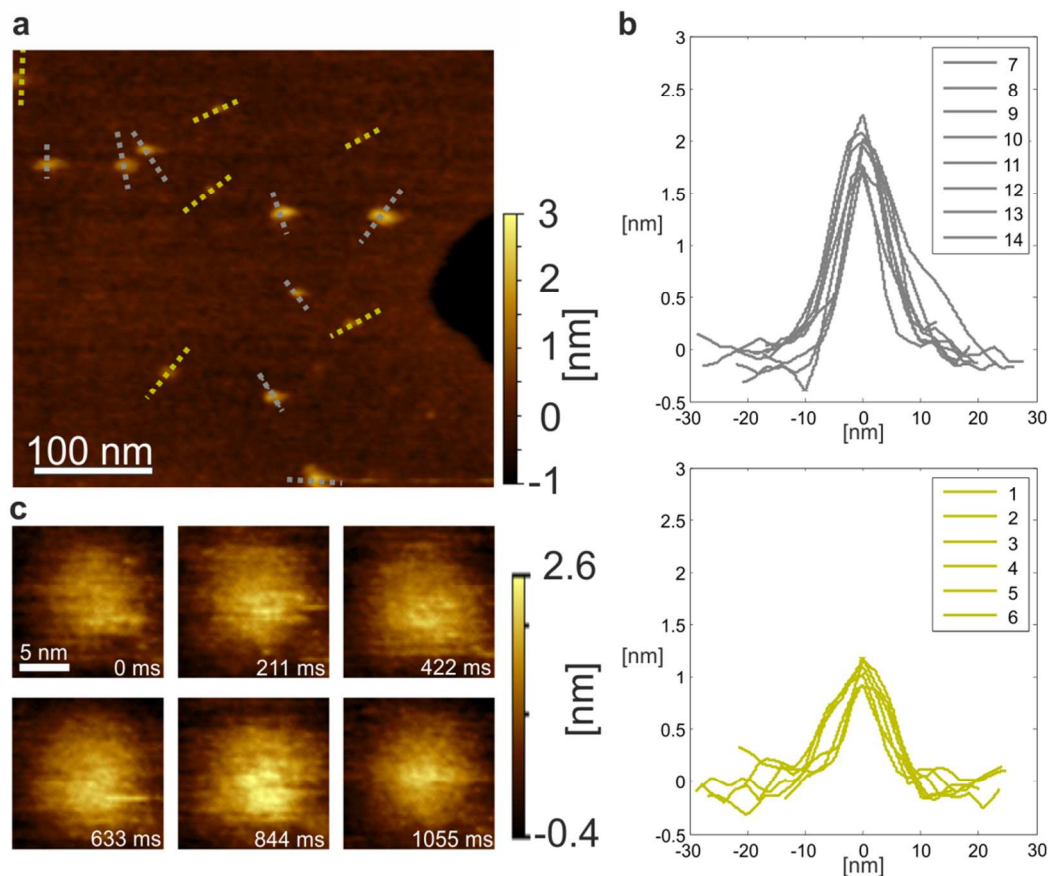


Figure S1 Orientation of AqpZ in supported lipid membranes. **(a)** AFM topograph of a supported lipid bilayer generated from vesicle fusion of AqpZ containing proteoliposomes. Two populations containing differently sized protrusions (indicated by yellow and grey lines, respectively) were observed with almost the same frequency of occurrence. **(b)** Cross section analysis along the grey (upper panel, cytoplasmic surface) and yellow (lower panel, periplasmic surface) dashed lines in (a). *Upper panel:* The height of the larger protrusions of ~ 2 nm can be rationalized by considering the N-terminal tails of AqpZ (20aa; 2.4 kDa, including the his-tag used for purification) located at the cytoplasmic surface^{1, 2}. Their volume (calculated from their molecular weight and specific volume of $0.73 \text{ cm}^3/\text{g}$ ³) corresponds to a protrusion size (when treated as a sphere) of ~ 2.3 nm. *Lower Panel:* The smaller sized protrusions of ~ 1 nm reflect the mean height taken from the periplasmic surface structures shown in Fig. 1c. **(c)** HS-AFM time series the cytoplasmic surface as observed in (a) reveals the weakly ordered protrusions

originating from the cytoplasmic 20aa N-terminal tail that mask the visualization of the underlying structure¹.

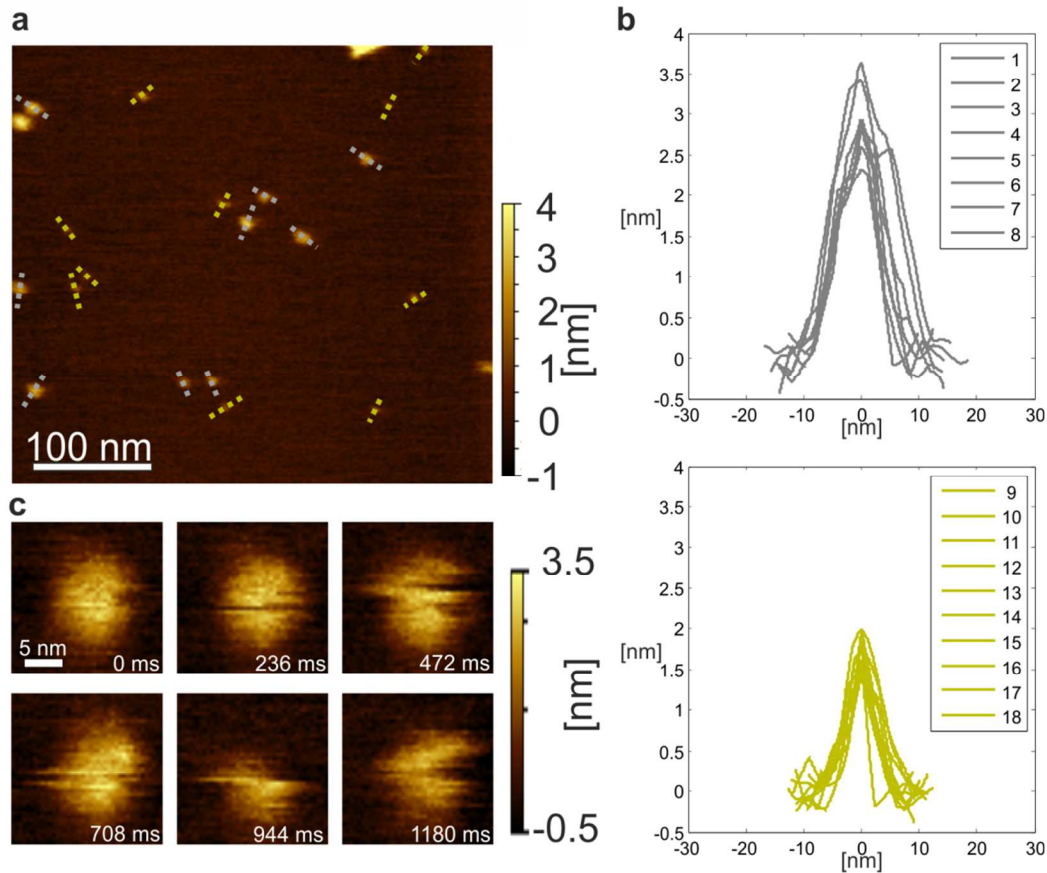


Figure S2 Orientation of GlpF in supported lipid membranes. **(a)** AFM topograph of a supported lipid bilayer generated from vesicle fusion of GlpF containing proteoliposomes. Two populations containing differently sized protrusions (indicated by yellow and grey lines, respectively) were observed with almost the same frequency of occurrence. **(b)** Cross section analysis along the grey (upper panel, cytoplasmic surface) and yellow (lower panel, periplasmic surface) dashed lines in (a). *Upper panel:* The height of the larger protrusions of ~ 2.5 nm can be rationalized by considering the N-terminal tails of GlpF (40aa; 3.9 kDa, including the his-tag used for purification) located at the cytoplasmic surface⁴. Their volume (calculated from their molecular weight and specific volume of $0.73 \text{ cm}^3/\text{g}^3$) corresponds to a protrusion size (when treated as a sphere) of ~ 2.8 nm. *Lower Panel:* The smaller sized protrusions of ~ 1.6 nm reflect the mean height taken from the periplasmic surface structures shown in Fig. 1b. **(c)** HS-AFM time series

the cytoplasmic surface as observed in (a) reveals the weakly ordered protrusions originating from the cytoplasmic 40aa N-terminal tail that mask the visualization of the underlying structure.

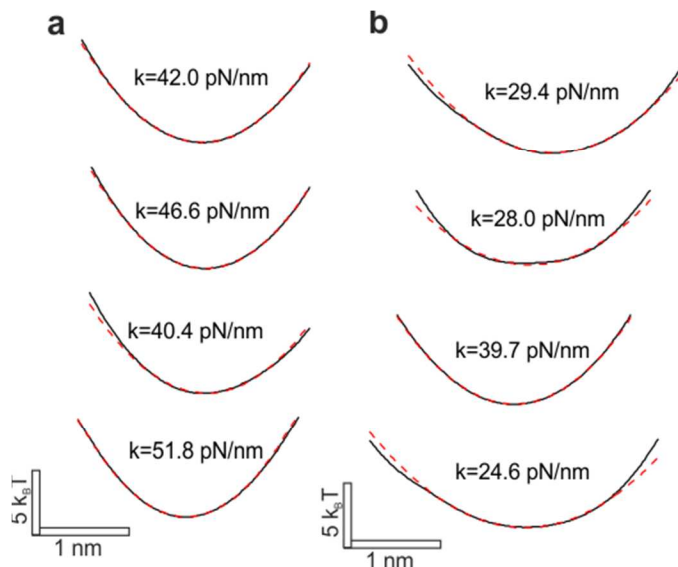


Figure S3 Determination of the loop stiffness k . **(a)** Examples of cross sections (black solid lines) taken through the energy landscape (GlpF, Figure 2c) and fits (red dashed lines) according to Eq. (3). **(b)** Examples of cross sections (black solid lines) taken through the energy landscape (AqpZ, Figure 2f) and fits (red dashed lines) according to Eq. (3).

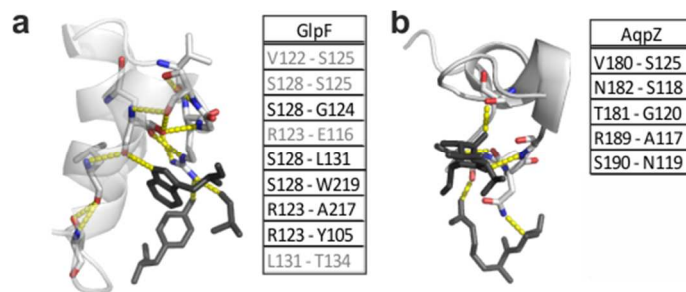


Figure S4 Polar contacts stabilizing GlpF and AqpZ loop C as suggested from crystal structure. **(a)** GlpF loop C viewed parallel to the membrane. Grey font color: 2 contacts; Black font color: 1 contact. **(b)** AqpZ loop C viewed parallel to the membrane. Polar contacts (tables) are sorted starting from the farthestmost (with respect to the membrane).

Movie S1 High speed AFM movie of GlpF recorded at 104 ms/frame. Scansize: 7.5 x 7.5 nm²; Color scale range 0 – 2 nm.

Movie S2 High speed AFM movie of AqpZ recorded at 104 ms/frame. Scansize: 7.5 x 7.5 nm²; Color scale range 0 – 1.3 nm.

References:

- (1) Scheuring, S.; Ringler, P.; Borgnia, M.; Stahlberg, H.; Müller, D. J.; Agre, P.; Engel, A. *EMBO J.* **1999**, 18, (18), 4981-4987.
- (2) Savage, D. F.; Egea, P. F.; Robles-Colmenares, Y.; O'Connell III, J. D.; Stroud, R. M. *PLoS Biol.* **2003**, 1, (3), e72.
- (3) Harpaz, Y.; Gerstein, M.; Chothia, C. *Structure* **1994**, 2, (7), 641-649.
- (4) Fu, D.; Libson, A.; Miercke, L. J.; Weitzman, C.; Nollert, P.; Krucinski, J.; Stroud, R. M. *Science* **2000**, 290, (5491), 481-486.